Second harmonic generation from Ge doped SiO2 (Gex(SiO2)1x) thin films grown by sputtering

Ibuki Kawamura, Kenji Imakita, Minoru Fujii, and Shinji Hayashi

Citation: Applied Physics Letters **103**, 201117 (2013); doi: 10.1063/1.4831984
View online: http://dx.doi.org/10.1063/1.4831984
View Table of Contents: http://scitation.aip.org/content/aip/journal/apl/103/20?ver=pdfcov
Published by the AIP Publishing

Re-register for Table of Content Alerts

Create a profile.
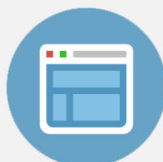
Sign up today!

This article is copyrighted as indicated in the abstract. Reuse of AIP content is subject to the terms at: http://scitation.aip.org/termsconditions. Downloaded to IP: 133.30.47.228 On: Sat, 30 Nov 2013 09:31:21

APPLIED PHYSICS LETTERS 103, 201117 (2013)

Second harmonic generation from Ge doped SiO_2 ($Ge_x(SiO_2)_{1-x}$) thin films grown by sputtering

Ibuki Kawamura, Kenji Imakita,[a)] Minoru Fujii, and Shinji Hayashi
Department of Electrical and Electronic Engineering, Graduate School of Engineering, Kobe University, Rokkodai, Nada, Kobe 657-8501, Japan

(Received 11 August 2013; accepted 1 November 2013; published online 15 November 2013)

Second-order nonlinear optical properties of sputter-deposited Ge-doped SiO_2 thin films were investigated. It was shown that the second-order nonlinearity of SiO_2, which vanishes in the electric-dipole approximation due to the centrosymmetric structure, can be significantly enhanced by Ge doping. The observed maximum value of d_{33} was 8.2 pm/V, which is 4 times larger than d_{22} of β-BaB_2O_4 crystal. Strong correlation was observed between the d_{eff} values and the electron spin resonance signals arising from GeP_b centers, suggesting that GeP_b centers are the most probable origin of the large second-order nonlinearity. © *2013 AIP Publishing LLC*.
[http://dx.doi.org/10.1063/1.4831984]

In recent years, nonlinear optical materials for silicon (Si) photonics have attracted significant attention. In particular, second order nonlinear optical material is of great interest toward the realization of CMOS-compatible electric optical modulators and frequency converters.[1–7] A lot of researches to induce second order nonlinearity to CMOS-compatible materials have been reported. For example, strong second harmonic generation (SHG) was observed from a Si waveguide on which a silicon nitride (SiN) layer was deposited.[8] The strain induced by the SiN layer to the waveguide causes the breakdown of the centrosymmetry of Si and brings about the large second-order nonlinearity. Ultraviolet (UV)-poled GeO_2 doped SiO_2 thin films are known to have large second order nonlinearity.[9–11] The origin is preferentially orientated polarization of oxygen vacancy defects, induced by the UV-poling process. Furthermore, a few kinds of amorphous thin films prepared by conventional deposition systems have been reported to exhibit large second order nonlinearity. For example, strong SHG signals were observed from SiN thin films prepared by plasma enhanced chemical vapor deposition, and silicon monoxide (SiO) thin films prepared by an electron beam deposition.[12,13] In these amorphous thin films, the origin of the second order nonlinearity has not been elucidated.

In this work, we propose Ge doped SiO_2 ($Ge_x(SiO_2)_{1-x}$) thin films as CMOS-compatible amorphous thin films that have large second-order nonlinearity. We show that the second-order nonlinearity of SiO_2, which vanishes in the electric-dipole approximation due to the centrosymmetric structure, can be significantly enhanced by the Ge doping ($Ge_x(SiO_2)_{1-x}$). The observed effective second-order nonlinear coefficient (d_{eff}) reaches as high as 5.48 pm/V. This value is more than twice larger than that of β-BaB_2O_4 (BBO). Electron spin resonance (ESR) measurements reveal that the thin films possess two kinds of oxygen vacancy defects, i.e., SiE′ and GeP_b centers. The comparison between the d_{eff} values and the ESR signal intensities demonstrates that GeP_b centers are the most possible origin of the large second-order nonlinearity of $Ge_x(SiO_2)_{1-x}$ thin films.

$Ge_x(SiO_2)_{1-x}$ thin films were prepared by a sputtering method. Small pieces of Ge tips ($4 \times 4\,mm^2$) and a SiO_2 wafer (10 cm in diameter) were used as sputtering targets. Ge concentration was controlled by the areal ratio of Ge to SiO_2 targets. Energy dispersive X-ray spectroscopy (EDS) measurements confirm that the Ge concentration ranges from 0 to 15.2 at. %. Fused silica plates were used as substrates. The film thickness was about 1 μm. X-Ray photoelectron spectroscopy (XPS) measurements were carried out with a fully automated XPS microprobe (PHI-Xtool, Ulvac-Phi, Japan) using Al Kα X-ray beam (1486.7 eV). Annealing was performed in a N_2 gas atmosphere. d_{eff} was estimated by analyzing SHG signals based on a Maker-fringe method. Figure 1 shows the optical setup. A mode-locked Ti:sapphire femtosecond laser with the wavelength of 800 nm and the full width of maximum (FWHM) of about 10 nm was used for the excitation. The pulse width and repetition frequency were 70 fs and 82 MHz, respectively. A monochromator equipped with a photomultiplier tube (PMT) was used to detect the SHG signal. The polarization of the excitation light was controlled by a Glanprism (GP) and a half-wave plate (HWP). A polarizer was placed in front of the monochromator to resolve the polarization of the SHG signal. Samples were set on a motorized rotation stage to change the incident angle (θ). Both the excitation and detection were p-polarized for the measurements of SHG spectra and Maker-fringe patterns. θ was set to $-50°$ for the estimation of d_{eff}. The refractive index (n) and extinction coefficient (k), which are necessary for the analysis of the SHG signal, were estimated from the transmittance (T) and reflectance (R) spectra. k at the wavelength of λ was obtained by using the relation $k = -(\lambda/4\pi L)\ln(T/(1-R))$, where L is the thickness of the thin films.[14] n was calculated by the relation $n = 1/2d(1/\lambda_n - 1/\lambda_{n+1})$, where λ_n is the peak wavelength of the nth peak in the interference fringe in the reflectance spectra of thin films.[15] BBO crystal was used as a reference sample whose d_{eff} is about 2.0 pm/V.[16] The second order nonlinear tensor components (d_{ij}) were estimated by analyzing the polarization dependence of SHG signals.[17,18]

Figures 2(a) and 2(b) show the Ge concentration dependence of Ge 3d and Si 2p XPS spectra for as-deposited

a)Electronic mail: imakita@eedept.kobe-u.ac.jp

 © 2013 AIP Publishing LLC

This article is copyrighted as indicated in the abstract. Reuse of AIP content is subject to the terms at: http://scitation.aip.org/termsconditions. Downloaded to IP: 133.30.47.228 On: Sat, 30 Nov 2013 09:31:21

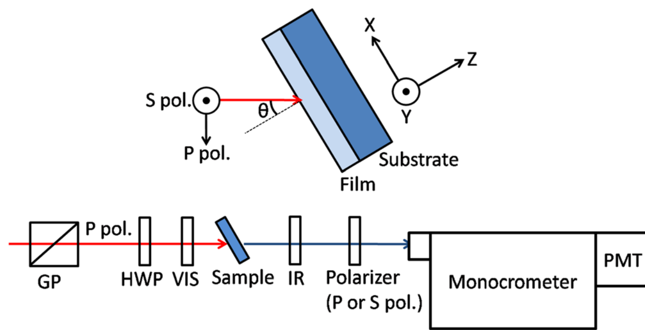

FIG. 1. Optical setup used for SHG measurements. GP, Glan prism; HWP, half-wave plate; VIS, visible-blocking filter; IR, infrared-blocking filter; PMT, photomultiplier tube.

$Ge_x(SiO_2)_{1-x}$. In Fig. 2(a), two peaks appear at 29.4 and 33.0 eV. These peaks correspond to Ge^0 and Ge^{4+}, respectively, indicating that Ge clusters and GeO_2 are simultaneously formed. In Fig. 2(b), a peak assigned to Si^{4+} can be seen at 103.2 eV. The peak energy is independent of Ge concentration, meaning that there are no Si-Ge bonds. Note that these results are very similar to those reported previously by other authors.[19] Figure 2(c) shows the Ge concentration dependence of the transmittance spectra. With increasing Ge concentration, the transmittance in the visible region decreases due to absorption by Ge clusters. On the other hand, high-transmittance of the near infrared region, which is important for applications in optical telecommunication, is preserved even for the sample with the highest Ge concentration.

Figure 3(a) shows Ge concentration dependence of the SHG spectra. For all the samples, we can see a peak at 400 nm with the FWHM of 4.5 nm. These values are the halves of those of the excitation light, confirming that the observed signals are the SHG of the excitation light. With increasing the Ge concentration, the SHG signal increases until the Ge concentration reaches 5.2 at. % and then decreases. When the Ge concentration is 0 at. %, the SHG signal is below the detection limit. Figure 3(b) shows Maker-fringe patterns as a function of Ge concentration. In all the patterns, the SHG intensity is negligible at 0°, and takes the maximum at −50° and 50°. This symmetric pattern is very similar to those observed for thin films with in-plane isotropy such as thermally poled optical glasses.[20,21] The left axis of Figure 3(c) shows the intensity of the observed SHG as a function of Ge concentration. It is the highest at 5.2 at. %. The decrease in the high Ge concentration region is partly due to large absorption at the SHG and excitation wavelengths. To eliminate the effect of the absorption, we estimated d_{eff} by using a formula taking into account the absorption.[17] The right axis of Figure 3(c) shows the d_{eff}. It increases with increasing Ge concentration, takes the maximum at 11.2 at. % and then decreases. The maximum value is 5.48 pm/V. This value is more than twice larger than that of BBO crystal.

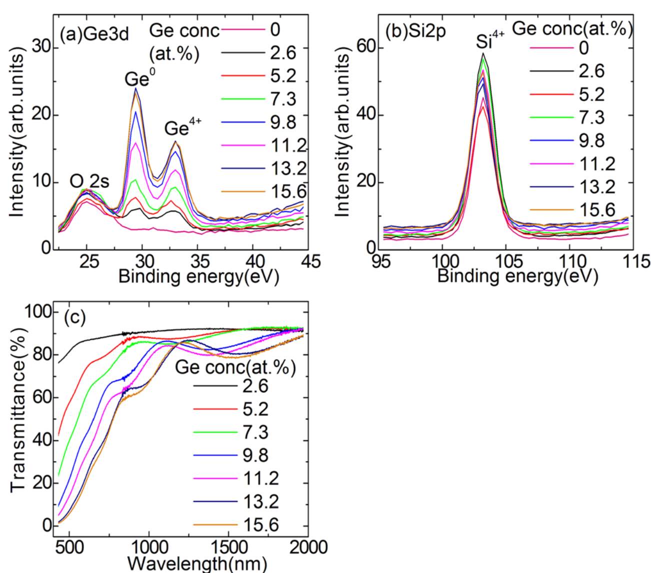

FIG. 2. Ge concentration dependence of XPS spectra in the (a) Ge 3d and (b) Si 2p regions for as-deposited $Ge_x(SiO_2)_{1-x}$ thin films with different Ge concentration. (c) Transmittance spectra of the as-deposited $Ge_x(SiO_2)_{1-x}$ thin films with different Ge concentration.

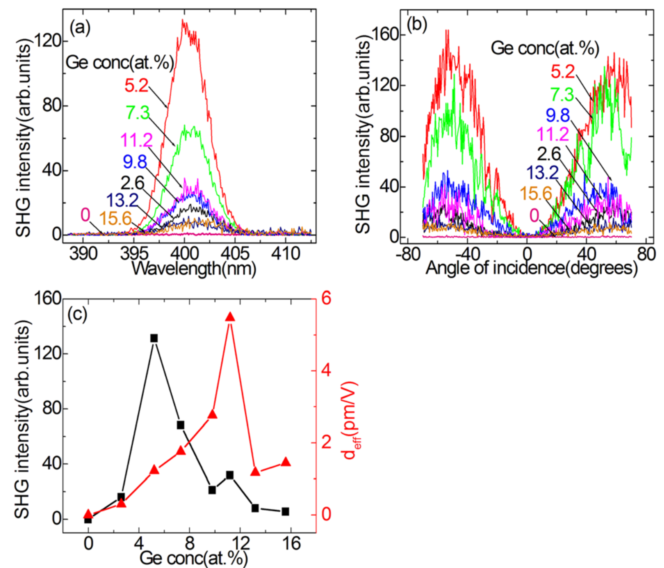

FIG. 3. (a) SHG spectra at θ of −50° and (b) Maker-fringe patterns, as a function of Ge concentration. (c) Ge concentration dependence of intensity of SHG (left-side) and d_{eff} (right-side).

Figure 4(a) shows the annealing temperature dependence of the transmittance spectra. The transmittance doesn't strongly depend on the annealing temperature, although it slightly decreases when the annealing temperature is 200 °C or 400 °C. Figure 4(b) shows the annealing temperature dependence of the SHG spectra. The SHG intensity decreases with increasing annealing temperature, and completely vanishes at 850 °C. Figure 4(c) shows the SHG and d_{eff} as a function of annealing temperature. Both the SHG intensity and d_{eff} decrease with increasing the annealing temperature. Similar results have been reported for SiN thin films.[18]

In general, there are two kinds of second-order nonlinearity, i.e., the bulk and interface nonlinearity. To determine them, we measured the thickness dependence of SHG spectra at the Ge concentration of 2.6 at. %. Figure 5(a) shows the result. The SHG intensity strongly depends on the film thickness. Figure 5(b) shows the SHG intensity as a function of the thickness. The dots and the solid line are the experimental and calculated results, respectively. The calculation assumes the bulk-type SHG response of absorptive

This article is copyrighted as indicated in the abstract. Reuse of AIP content is subject to the terms at: http://scitation.aip.org/termsconditions. Downloaded to IP: 133.30.47.228 On: Sat, 30 Nov 2013 09:31:21

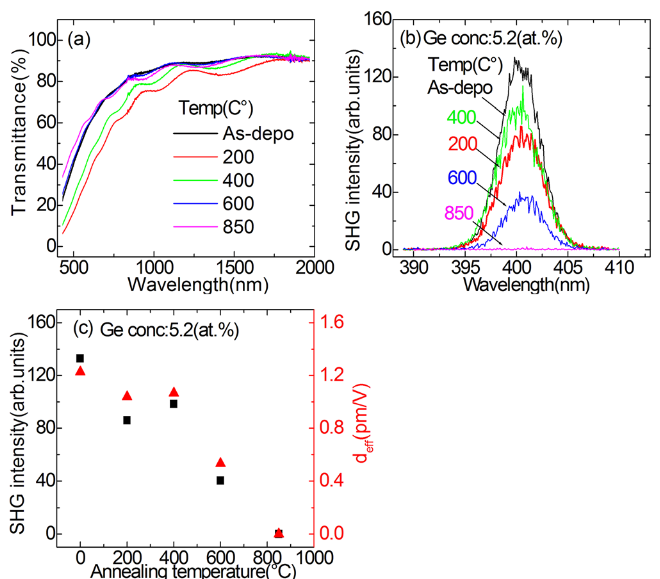

FIG. 4. Annealing temperature dependence of (a) transmittance spectra, (b) SHG spectra at θ of $-50°$, and (c) intensity of SHG (left-side) and d_{eff} (right-side) at the Ge concentration of 5.2 at. %.

thin films.[17] The SHG intensity increases with increasing the film thickness, and the experimental result is well reproduced by the calculation. This suggests that the bulk second order nonlinearity is responsible for the observed SHG. There are several possible origins as bulk second order nonlinearity of our samples. One of them is Ge clusters. If the polarization of the Ge clusters is preferentially oriented, they can induce the second order nonlinearity. Similar discussion can be seen in the previous report on the SHG from Si-rich SiN, in which Si clusters are suggested as the possible origin.[12] However, this model cannot explain the decrease of d_{eff} in the high Ge concentration region in Fig. 3(c). The second one is oxygen vacancy defects. In case of UV-poled GeO_2 doped SiO_2 thin films, preferentially oriented oxygen vacancy defects (GeE′ centers) induce the second order nonlinearity. Figure 6(a) shows the ESR signals as a function of Ge concentration. The solid curves are the results of the fitting by two Gaussian functions. The g values of the two peaks are 2.004 and 2.019, which can be assigned to SiE′ and GeP_b centers, respectively.[22–24] Note that the signal from GeE′ center, g value of which is 1.995 (Ref. 25) (351.9 mT in Fig. 6(a)), is not observed. This is in sharp contrast with UV-poled GeO_2 doped SiO_2 (germanosilicate glass), in which GeE′ centers are the dominant oxygen vacancy defects.[9,26] Figure 6(b)

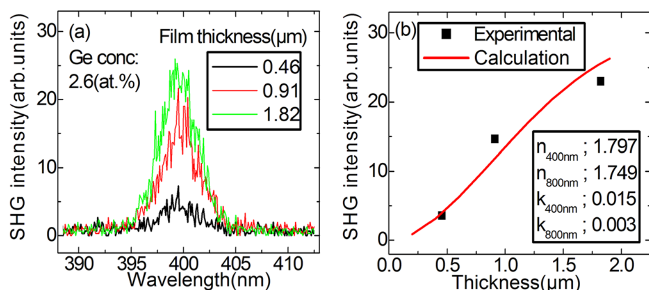

FIG. 5. (a) Film thickness dependence of SHG spectra at θ of $-50°$ at the Ge concentration of 2.6 at. %. (b) Experimental (dots) and calculated (solid line) SHG intensity as a function of film thickness.

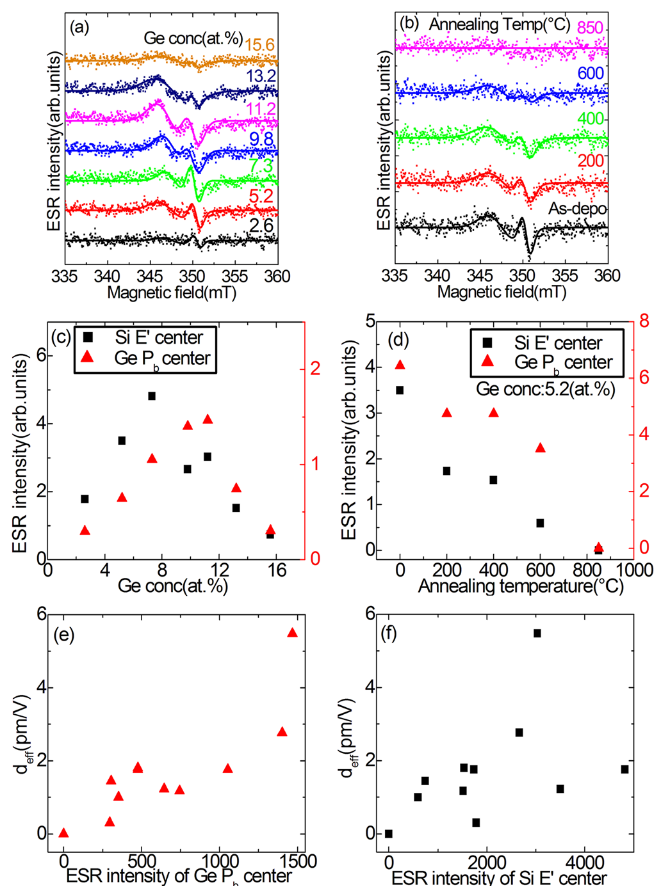

FIG. 6. X-band ESR signals of (a) as-deposited $Ge_x(SiO_2)_{1-x}$ thin films as a function of Ge concentration and (b) annealing temperature at room temperature at the Ge concentration of 5.2 at. %. The intensity of SiE′ center (left-side) and GeP_b center (right-side) as a function of (c) Ge concentration and (d) annealing temperature at the Ge concentration of 5.2 at.%. d_{eff} as a function of the ESR signal intensity of (e) GeP_b centers and (f) Si E′ centers.

shows X-band ESR signals as a function of annealing temperature. We can see that the ESR signal intensity depends strongly on the annealing temperature. Figure 6(c) plots the intensity of the ESR peaks as a function of Ge concentration. With increasing Ge concentration, the intensities of GeP_b and SiE′ centers increase and then decrease. The intensity of GeP_b centers takes the maximum at 11.2 at. %, while that of SiE′ centers does at 7.3 at. %. Figure 6(d) shows the annealing temperature dependence of the ESR signal intensities of GeP_b and SiE′ centers. Both of them decrease with increasing the annealing temperature. In Figs. 6(e) and 6(f), d_{eff} are plotted as a function of the ESR signal intensities of GeP_b and SiE′ centers, respectively. We can see correlations between the d_{eff} value and the ESR signal intensities in Figs. 6(e) and 6(f). Furthermore, the correlation coefficients of Figs. 6(e) and 6(f) are 0.83 and 0.45, respectively. The results suggest that the GeP_b centers are more probable origin of the second-order nonlinearity of $Ge_x(SiO_2)_{1-x}$ thin films. It should be stressed here that the second-order nonlinearity should not appear if the material possesses inversion symmetry. The observed large second order nonlinearity suggests that the inversion symmetry of the $Ge_x(SiO_2)_{1-x}$ thin films is broken during the deposition process. The mechanism of the preferential orientation of GeP_b centers is not clear.

This article is copyrighted as indicated in the abstract. Reuse of AIP content is subject to the terms at: http://scitation.aip.org/termsconditions. Downloaded to IP: 133.30.47.228 On: Sat, 30 Nov 2013 09:31:21

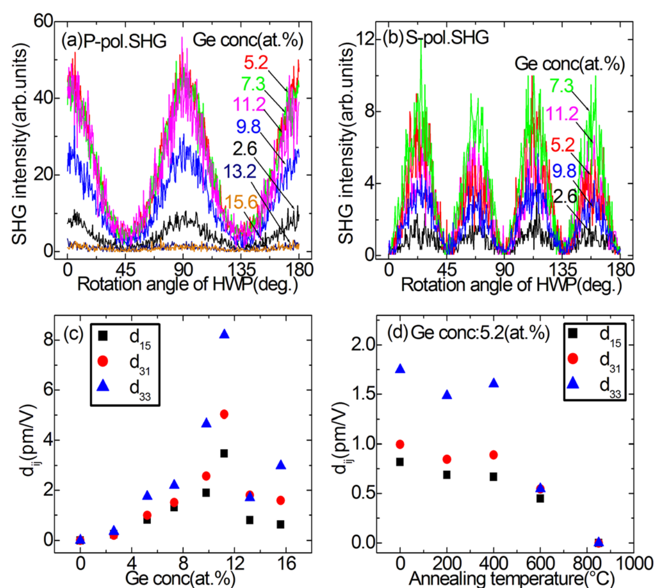

FIG. 7. (a) p- and (b) s-polarized SHG signal as a function of rotation angle of HWP. The rotation angles of 0° (or 90°, 180°) and 45° (or 135°) correspond to the P- and S-polarization of the excitation light. The θ was $-50°$. The tensor components of d_{15}, d_{31}, and d_{33} as a function of (c) Ge concentration and (d) annealing temperature at the Ge concentration of 5.2 at. %.

Figures 7(a) and 7(b) show the p- and s-polarized SHG intensity as a function of the rotation angle of the HWP in Fig. 1. The rotation angles of 0° (or 90°, 180°) and 45° (or 135°) correspond to the p- and s-polarization of the excitation light, respectively. We find that both p- and s-polarized SHG signal intensities strongly depend on the polarization of the excitation light. In Fig. 7(a), we see that the p-polarized SHG intensity takes a maximum (minimum) when the excitation light is p (s) -polarized. On the other hand, in Fig. 7(b), the s-polarized SHG signals become zero in the case of p- and s-polarization of the excitation light. To analyze these data, we assume that the thin films possess in-plane symmetry ($C_{\infty v}$ symmetry group). The assumption is plausible considering the fact that the thin films are vertically deposited on isotropic silica substrates. In fact, The Maker-fringe patterns in Fig. 3(a) and the polarization dependence in Fig. 7(b) are consistent with the results predicted for thin films belonging to the $C_{\infty v}$ symmetry group.[12,27] In this symmetry group, the second-order nonlinear tensors have three independent tensor components of d_{15}, d_{31}, and d_{33}.[28] Figures 7(c) and 7(d) show the tensor components as a function of Ge concentration and annealing temperature. All the tensor components show dependence similar to that of d_{eff} shown in Figs. 3(c) and 4(c). For all the samples, d_{33} is the largest and d_{15} is the smallest. This result is similar to those previously reported for thin films belonging to the $C_{\infty v}$ symmetry group and implies the breakdown of the inversion symmetry in the z-axis.[12,25,29] The maximum value of d_{33} is 8.2 pm/V at 11.2 at.%. This is about 4 times larger than d_{22} of BBO crystal, and comparable to d_{33} of UV-poled GeO_2 doped SiO_2 thin films (12.5 pm/V).[9]

In conclusion, we observed strong SHG from $Ge_x(SiO_2)_{1-x}$ thin films prepared by sputtering. The maximum value of d_{33} was 8.2 pm/V, which is about 4 times larger than d_{22} of BBO crystal. The comparison between the d_{eff} values and the ESR signal intensities suggests that the possible origin of the large second-order nonlinearity is GeP_b centers. Our results suggest that $Ge_x(SiO_2)_{1-x}$ thin films are a promising material for second-order nonlinear optical devices which can be used in silicon photonics.

This work was supported by KAKENHI (23310077).

[1]J. Leuthold, C. Koos, and W. Freude, Nat. Photonics **4**, 535 (2010).
[2]J. Y. Lee, L. Yin, G. P. Agrawal, and P. M. Fauchet, Opt. Express **18**, 11514 (2010).
[3]P. Mehta, N. Healy, T. D. Day, J. R. Sparks, P. J. A. Sazio, J. V. Badding, and A. C. Peacock, Opt. Express **19**, 19078 (2011).
[4]K. Mukherjee, P. Ghosh, D. Kumbhakar, and A. K. Meikap, Opt. Quant. Electron. **42**, 121–128 (2010).
[5]T. Tanabe, M. Notomi, S. Mitsugi, A. Shinya, and E. Kuramochi, Appl. Phys. Lett. **87**, 151112 (2005).
[6]H. K. Tsang and Y. Liu, Semicond. Sci. Technol. **23**, 064007 (2008).
[7]H. Jelínková, J. Šulc, P. Koranda, M. Němec, M. Čech, M. Jelínek, and V. Škoda, Laser Phys. Lett. **1**, 59 (2004).
[8]M. Cazzanelli, F. Bianco, E. Borga, G. Pucker, M. Ghulinyan, E. Degoli, E. Luppi,V. Veniard, S. Ossicini, D. Modotto, S. Wabnitz, R. Pierobon, and L. Pavesi, Nature Mater. **11**, 148 (2012).
[9]J. Khaled, T. Fujiwara, M. Ohama, and A. J. Ikushima. J. Appl. Phys. **87**, 2137 (2000).
[10]T. Fujiwara, T. Sawada, T. Honma, Y. Benino, T. Komatsu, M. Takahashi, T. Yoko, and J. Nishi, Jpn. J. Appl. Phys., Part 1 **42**, 7326 (2003).
[11]T. Fujiwara, M. Takahashi, and A. J. Ikushima, Appl. Phys. Lett. **71**, 1032 (1997).
[12]T. Ning, H. Pietarinen, O. Hyvärinen, J. Simonen, G. Genty, and M. Kauranen, Appl. Phys. Lett. **100**, 161902 (2012).
[13]S. V. Andersen and K. Pedersen, Opt. Express **20**, 13857 (2012).
[14]T. Kamiya, K. Nomura, M. Hirano, and H. Hosono, Phys. Status Solidi C **5**, 3098 (2008).
[15]C. Pickering, M. I. J. Beale, and D. J. Robbins, Thin Solid Films **125**, 157 (1985).
[16]D. N. Nikogosyan, Appl. Phys. A **52**, 359 (1991).
[17]W. N. Herman and L. M. Hayden, J. Opt. Soc. Am. B **12**, 416 (1995).
[18]E. F. Pecora, A. Capretti, G. Miano, and L. Dal Negro. Appl. Phys. Lett. **102**, 141114 (2013).
[19]A. G. Rolo, O. Conde, M. J. M. Gomes, and M. P. Santos, J. Mater. Process. Technol. **92–93**, 269 (1999).
[20]M. Dussauze, T. Cremoux, F. Adamietz, V. Rodriguez, E. Fargin, G. Yang, and T. Cardinal, Int. J. Appl. Glass Sci. **3**, 309 (2012).
[21]M. Dussauze, E. Fargin, M. Lahaye, V. Rodriguez, and F. Adamietz, Opt Express **13**, 4064 (2005).
[22]K. Toshikiyo, M. Tokunaga, S. Takeoka, M. Fujii, and S. Hayashi, J. Appl. Phys. **89**, 4917 (2001).
[23]M. Ito, K. Imakita, M. Fujii, and S. Hayashi, J. Appl. Phys. **108**, 063512 (2010).
[24]A. Stesmans, P. Somers, and V. V. Afanas'ev, Phys. Rev. B **79**, 195301 (2009).
[25]J. Nishii, Mater. Sci. Eng., B **54**, 1 (1998).
[26]M. Takahashi, T. Fujiwara, T. Kawachi, and A. J. Ikushima, Appl. Phys. Lett. **71**, 993 (1997).
[27]S. Lettieri, S. Di Finizio, P. Maddalena, V. Ballarini, and F. Giorgis, Appl. Phys. Lett. **81**, 4706 (2002).
[28]N. Okamoto, Y. Hirano, and O. Sugihara, J. Opt. Soc. Am. B **9**(11), 2083 (1992).
[29]D. F. Logan, A. B. A. Dow, D. Stepanov, P. Abolghasem, N. P. Kherani, and A. S. Helmy, Appl. Phys. Lett. **102**, 061106 (2013).

This article is copyrighted as indicated in the abstract. Reuse of AIP content is subject to the terms at: http://scitation.aip.org/termsconditions. Downloaded to IP: 133.30.47.228 On: Sat, 30 Nov 2013 09:31:21